

Entwicklung von Messmethoden  
in der  
Spektrophotometrie

Development of methods  
for spectrophotometrical  
measurements

von  
Valentin Reinhardt

Bachelorarbeit in Physik

angefertigt im  
Institut für Methodik der Fernerkundung  
am Deutschen Zentrum für Luft- und Raumfahrt

vorgelegt der

Fakultät für Physik  
an der Ludwig-Maximilians-Universität  
München  
im August 2013

Erstprüfer: Prof. Dr. Bernhard Mayer  
Betreuer: Karim Lenhard



# Contents

<b>Introduction</b>	<b>5</b>
<b>1 Principles</b>	<b>7</b>
1.1 Definitions . . . . .	7
1.1.1 Intensity . . . . .	7
1.1.2 Transmittance . . . . .	7
1.1.3 Absorbance . . . . .	8
1.1.4 Reflectance . . . . .	8
1.2 Measurement principle of a double beam spectrophotometer . . . . .	8
1.3 The Perkin Elmer Lambda 1050 Spectrophotometer . . . . .	11
1.4 Cary Win UV Spectrophotometer . . . . .	14
1.5 Potential error sources . . . . .	14
1.5.1 Polarization . . . . .	14
1.5.2 Homogeneity of detector and light beam . . . . .	16
1.5.3 Optical paths . . . . .	16
1.5.4 Noise . . . . .	18
1.5.5 Aging of the reflection standards . . . . .	18
<b>2 Methods</b>	<b>19</b>
2.1 Common Beam Mask . . . . .	19
2.2 Transmission measurements . . . . .	19
2.2.1 Reproducibility . . . . .	20
2.2.2 Polarization . . . . .	20
2.3 Reflection measurements . . . . .	21
<b>3 Results</b>	<b>25</b>
3.1 Experimental experiences . . . . .	25
3.1.1 Reflection problems . . . . .	25
3.1.2 Stray light problems . . . . .	27
3.1.3 Detector change . . . . .	27
3.2 Common Beam Mask . . . . .	28

3.3	Reproducibility of transmittance measurements . . . . .	30
3.4	Filter transmission . . . . .	31
3.5	Polarization . . . . .	36
3.6	Reflection measurements . . . . .	39
<b>4</b>	<b>Conclusion &amp; Outlook</b>	<b>43</b>
	<b>Literaturverzeichnis</b>	<b>43</b>

# Introduction

The Remote Sensing Technology Institute (IMF) of the German Aerospace Center (DLR) in Oberpfaffenhofen engages in hyperspectral remote sensing of the environment. Remote sensing provides data from bio-geophysical properties for large areas, which are used as input parameters for a multitude of bio-geophysical models, see [SC01]. As the quality of these models depends on the quality of the data, the instruments collecting the data have to be calibrated thoroughly. For this purpose, the IMF department Experimental Methods operates a calibration facility for optical spectrometers, the Calibration Home Base, see [GE01]. Hyperspectral sensors (such as the Airborne Prism Experiment [GE01]) operating in a wavelength range of 350 nm to 2550 nm are calibrated there.

Some calibration methods use filters and diffuse reflectance samples (spectralons). Filters are used to calibrate detectors for hyperspectral airborne experiments and spectralons are a source for the white balancing of field spectroradiometers. It is desirable, that the qualities of the calibration samples are known as precisely as possible.

To characterize these filters and spectralons, a new double beam spectrophotometer Lambda 1050 of Perkin Elmer Industries, which has not been used yet, is available as well as an older device from Varian. These spectrophotometers are able to measure reflection and transmission qualities of samples as a function of wavelength. For the calibration tasks, the spectrophotometers must be able to deliver precise and reproducible measurement results. Therefore, the properties of the new Lambda device must be studied and measurement methods must be established.

During my work at DLR, I characterized the new Perkin Elmer Lambda 1050 spectrophotometer for transmission and reflection measurements and developed measurement methods yielding appropriate results. To accomplish these tasks, I used a set of ten filters and two spectralons, which were calibrated already by the national metrological institutes of the UK and the U.S. This information was very helpful for validating my methods and the assessment of uncertainties of the DLR measurements. The results of my work are presented on the following pages and the Perkin Elmer Lambda 1050 Spectrophotometer is now ready for use as calibration instrument for DLR tasks.

The methods can be found in chapter 2. The measurements also revealed some common mistakes which are discussed at the beginning of the results section.

# Chapter 1

## Principles

A short introduction into the spectrophotometer and its related components and definitions will be given, before the characterisation methods are explained.

### 1.1 Definitions

#### 1.1.1 Intensity

The Intensity  $I$  of light is an energy unit. It is defined as:

$$I = \frac{\text{Energy}}{\text{Area} \times \text{Time}} \quad \text{with the unit} \quad \left[ \frac{W}{m^2} \right] \quad (1.1)$$

This intensity can be measured directly by a detector and is thereby integrated over a time period.

#### 1.1.2 Transmittance

If a collimated light beam is directed towards a sample, the transmission  $T$  is defined as the fraction which passes through. It can be derived directly from the relation of intensities.  $I_0$  is the incident intensity and  $I_T$  the transmitted intensity. Transmittance values range from 0 to 1 and are given in this work in as:

$$\% T = \frac{I_T}{I_0} \times 100 \% \quad (1.2)$$

### 1.1.3 Absorbance

The absorbance  $A$  is a parameter to quantify the absorption process. It can be derived from the transmission by the decadic logarithm

$$A = -\log_{10} \left( \frac{I_T}{I_0} \right). \quad (1.3)$$

### 1.1.4 Reflectance

Reflectance  $R$  is the fraction of incident light which is reflected. It can also be derived by comparison of the intensities.  $I_R$  is the reflected intensity. Reflectance values, like transmittance values, range from 0 to 1 and are specified in this work as reflectance factor  $R$ .

$$R = \frac{I_R}{I_0} \quad (1.4)$$

The direction of reflected light is dependent on the reflecting material and can vary between two extrema which are called specular and diffuse reflection:

Specular reflection obeys Snell's law stating incidence angle is equal to the reflectance angle [RA01].

Diffuse reflection obeys Lambert's law: "The light from a lambertian reflector is distributed uniformly over the hemisphere" [RA01].

## 1.2 Measurement principle of a double beam spectrophotometer

In a spectrophotometer, the intensities of two narrowband light beams, which come from the same source but have split up, are compared by one detector at different wavelengths. One beam contains a test sample and is called: "Sample beam". The other one is called "reference beam".

At first, a reference measurement is done without any sample. This is to quickly calibrate the detector, hereby eliminating mathematically any differences between the two signals. Thereafter, the sample is brought into the path of one beam. The spectrophotometer continuously compares the two light beams. The relation of the two detected intensities gives directly the transmission % T as a function of wavelength, which can be transformed to absorbance. Reflectance is measured by choosing a sample set-up in which the reflected light is directed to the detector. An example is described in section 1.3.



1.2. MEASUREMENT PRINCIPLE OF A DOUBLE BEAM SPECTROPHOTOMETER<sup>9</sup>

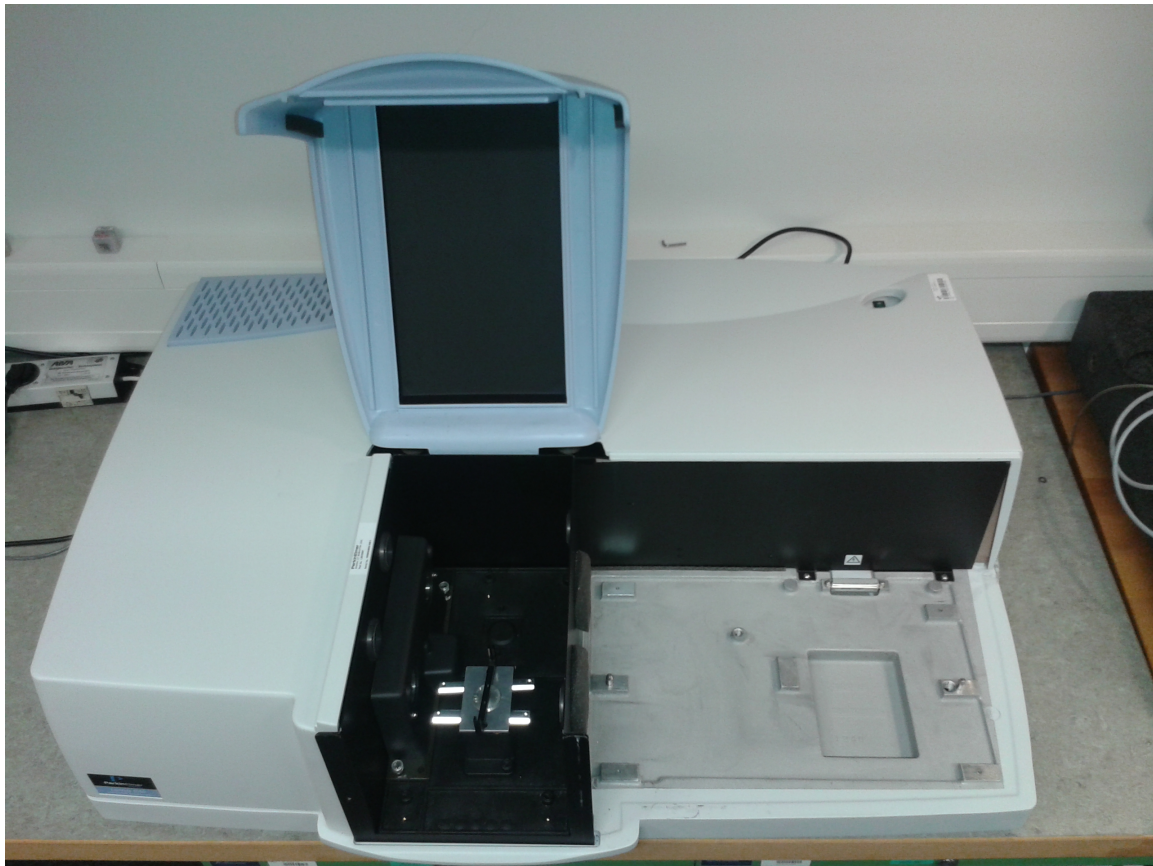


Figure 1.1: Photo of the Perkin Elmer Lambda 1050 Spectrophotometer with the sample compartment open and no detector module installed.

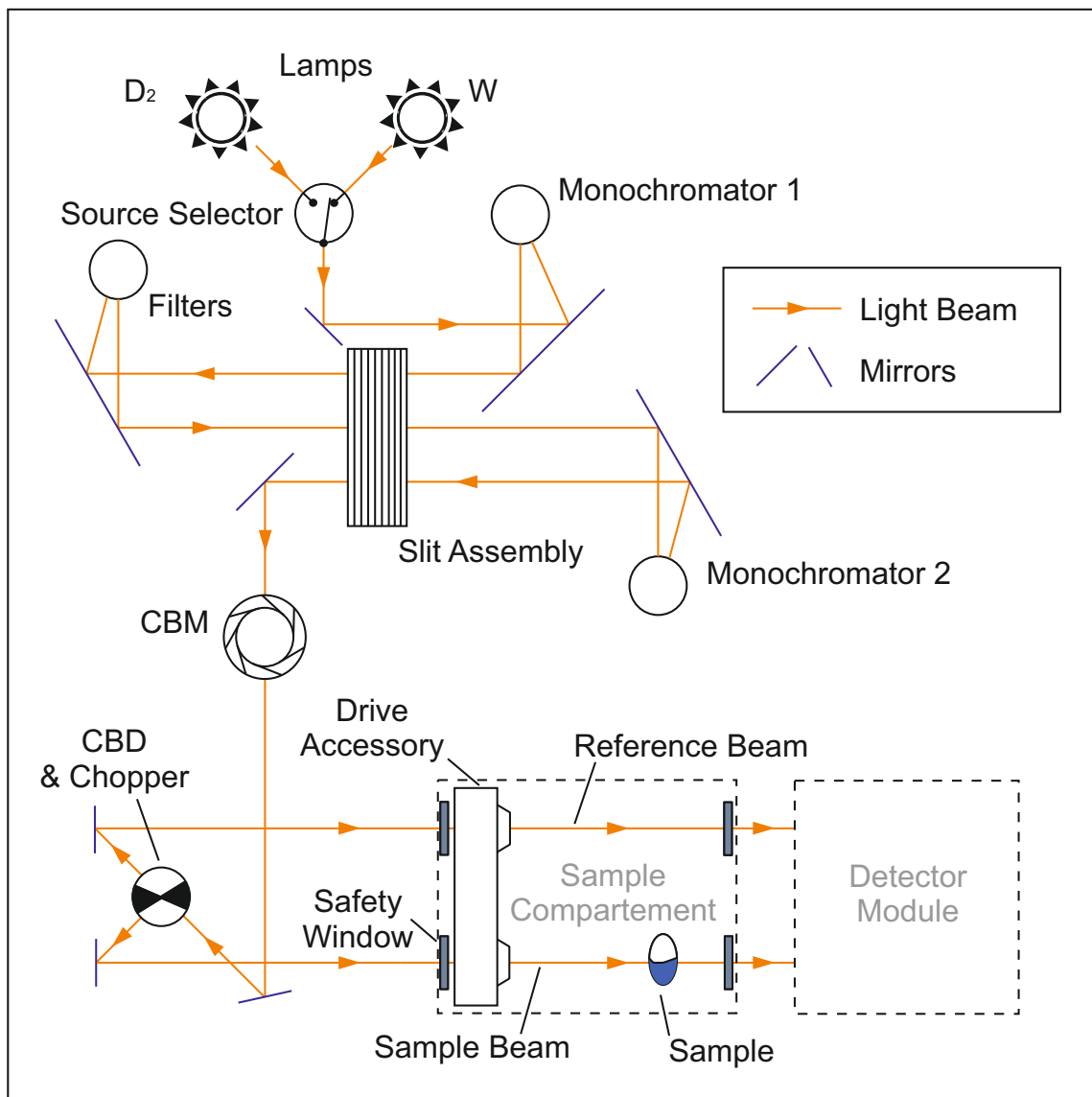


Figure 1.2: Path of light through the schematic setup of the Perkin Elmer Lambda 1050 Spectrophotometer. The light is emitted either by the deuterium lamp ( $D_2$ ) or the tungsten lamp (W). The CBM is the Common Beam Mask and the CBD the Common Beam Depolarizer.

## 1.3 The Perkin Elmer Lambda 1050 Spectrophotometer

The Perkin Elmer Lambda 1050 spectrophotometer is a double beam spectrophotometer and is shown in figure 1.1. Figure 1.2 shows the path of light through a schematic setup. Measurements can be made in a spectral range from 175.0 nm to 3300.0 nm, which is covered by two lamps. A deuterium lamp  $D_2$  for the ultraviolet (UV) section and a tungsten lamp W for the visible (VIS) and near infrared (NIR) spectral regions. The tungsten lamp produces, as all incandescent light bulbs, a continuous spectrum from the near UV throughout the rest of the spectral range. The wavelength where the lamps as light-source are swapped by the source selector can be chosen between 300 and 350 nm. The deuterium lamp emits a continuous spectrum from 160 nm to 400 nm.

The light is imaged through a slit assembly towards a set of filters and two consecutive monochromators which use holographic gratings. From the incoming light these monochromators filter a fraction with a small bandwidth. The amount of stray light, i.e. light at wavelengths other than the defined bandwidth is reduced to a minimum ( $> 0.00007\%$  [PE01]). According to the manufacturer, the slit assembly can be adjusted by the software to allow a resolution of the measured spectrum of at least 0.05 nm in the UV/VIS range and 0.20 nm in the NIR region [PE01]. This is due to the different gratings used for each spectral region. The gratings of the UV/VIS monochromators have four times more lines per mm, which results in a four times higher resolution.

The light beam continues through a mask (Common Beam Mask, CBM), which is able to set the spot size from a maximum of 10.9 mm to 0 mm. Thereafter, a depolarizer crystal (Common Beam Depolarizer, CBD) follows, which can be included in the measurement if required. Afterwards, the light beam is separated into the reference beam and the sample beam by a chopper, consisting of a rotating disc with a mirror and a window segment directing the beam in either direction. The two beams are then directed through the sample compartment of the spectrophotometer, where the samples can be placed in either path. Within the compartment a drive accessory is installed, just in front of the samples, which can hold and rotate a polarizing or depolarizing crystal. At the detector compartment, different detectors can be installed. Three different detector modules are available for this work:

### Three Detector Module

This module directs light depending on the spectral range of the wavelengths, through a mirror translation unit, to one of the three detectors. The exact handover wavelengths can be selected within the software.

The first detector for the a spectral range from the UV region up to around 850 nm is a Photo Multiplier Tube (PMT).

The second detector for signals up to 1800 nm is a Indium-Gallium-Arsenide detector (InGaAs).

The third detector is a lead sulphide (PbS) photo diode-type detector covering the range from 1800 nm to the end of the spectrometer's spectral range at 3300 nm.

### Sphere module

The sphere module is able to measure the transmission of diffusely scattering or polarizing samples, as well as the reflectance of a sample. Its main element is an integrating sphere with a diameter of 150 mm which can be seen in figure 2.1 or schematically in figure 1.3. The sphere is coated on the inside with a nearly perfectly white and diffuse reflecting material made out of Polytetrafluoroethylene ( $(C_2F_4)_n$ ). Light entering the sphere will be reflected on its walls many times before it encounters the detector. This has the advantage that the detector will produce a signal proportional to all light entering the sphere in contrast to the three detector module, where only the light in the direction of the detector is measured. Thus, all the transmitted light from a sample if placed directly in front of the sphere can be measured.

Diffuse reflectance measurements can be made by putting a sample where the entering sample beam first meets the far end of the sphere. Again, all the reflected light from this diffusely reflecting sample will be measured.

Since the integrating sphere allows for a diffuse and homogeneous illumination of the detector, potential measurement errors due to beam shape, polarization or other beam qualities are suppressed.

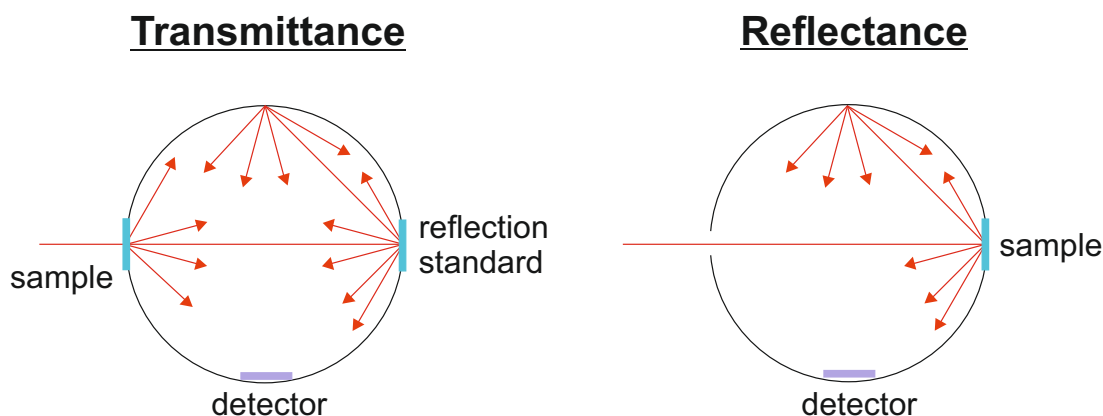


Figure 1.3: Measurement principles with the sphere module for the sample beam. The reference beam is not shown.

The sphere has six ports, some of which can be closed by covers coated with the same white material: Two ports for the sample and reference beam to enter the sphere, one at the end for the reflectance sample, one at the bottom where the detectors are placed and one at the top to put a sample from above with a hanger inside the sphere. The last one is located at a position where the specular reflected light from a sample at the far end would hit the sphere. Thus, if opened, specular reflectivity can be measured separately from diffuse one.

The detector unit of this module consists only of two detectors (PMT, PbS), which means it is able to detect infrared light up to 3300 nm, but with a reduced signal to noise ratio for high absorbance samples as the InGaAs detector is missing, according to the manufacturer [PE01]. For a definition of the signal to noise ratio, see section 1.5.4.

### Universal Reflectance module

The universal reflectance module (URA) measures the specular reflectance of a sample for different incident angles. For this, the detector is placed on a gantry which also bears mirrors for a correct alignment of the sample beam. The angle of incidence can be varied from  $8^\circ$  to  $65^\circ$  in steps of  $0.5^\circ$ .

### Slits

The slits control the resolution of the measurements and the light intensity within the beams. These variables are within the spectrophotometer complementary to each other, which for example means, that for an increase in resolution the intensity of light is reduced. Each detector requires a different operating range for the intensity of light, which also depends on the wavelength. Therefore the slit setting is important for a usable result. In the software only the required bandwidth can be set. The slit width is then set accordingly by the software. For the PMT detector range, the slit is fixed and the bandwidth can be set from 0.05 nm to 5 nm in steps of 0.5 nm.

For the infrared detectors the slits are either fixed, with spectral bandwidths ranging from 0.2 nm to 20 nm in steps of 0.2 nm, or variable, meaning that the slit is controlled by the software in the above mentioned range. In this case, the software will choose the bandwidths so that the detector can operate properly. With this setting, it is not possible to explicitly specify the resolution.

To correct for low intensities and thus allow high resolution results with a high signal to noise ratio, there are two more possibilities:

- The detector signal can be amplified with the disadvantage of a decreasing signal to noise ratio. Perkin Elmer [PE04] recommends the following minimum gain settings in the software, which is described in the next section:

<b>Detector</b>	<b>NIR gain</b>
PbS	1
InGaAs, no sphere	5
InGaAs, with sphere	14

- The integration time of the detector signal can be prolonged. It is selectable between 0.04s, which is the minimum chopper cycle, and 10.00s. Hereby, the duration of the measurement and the signal to noise ratio increase.

## Software

The spectrophotometer is controlled by a Perkin Elmer software called UV WinLab. Figure 1.4 shows a screenshot. Within the software, all settings are defined such as spectral range, resolution, gain, switching the reference and the sample beam, CBD activation. The results are transferred to the computer with an accuracy of 6 decimals (A or %T). The results can be exported as .csv or .asc file but in the .csv-file the data are rounded to only 2 decimals. A defined set of parameters can be saved as method. With these methods, measurements can quickly be started without the need of doing all settings again.

## 1.4 Cary Win UV Spectrophotometer

The set-up of the old DLR spectrophotometer Cary1 is similar to the new one but it is missing a few features: The Cary 1 measures transmission from 190 nm to 900 nm. It has only one monochromator and no additional detectors. Reflection measurements need to be installed in the sample compartment.

## 1.5 Potential error sources

This section will give background information on errors which are typical for measurements with a double beam spectrophotometer.

### 1.5.1 Polarization

Within the optics of the spectrophotometer, the light which, emitted by the incandescent electric lamps or gas discharge lamps, is naturally non-polarized [LA01], will get polarized to a certain amount. The main causes for polarization are:

- reflections on the mirrors, and
- the diffraction gratings within the monochromator.

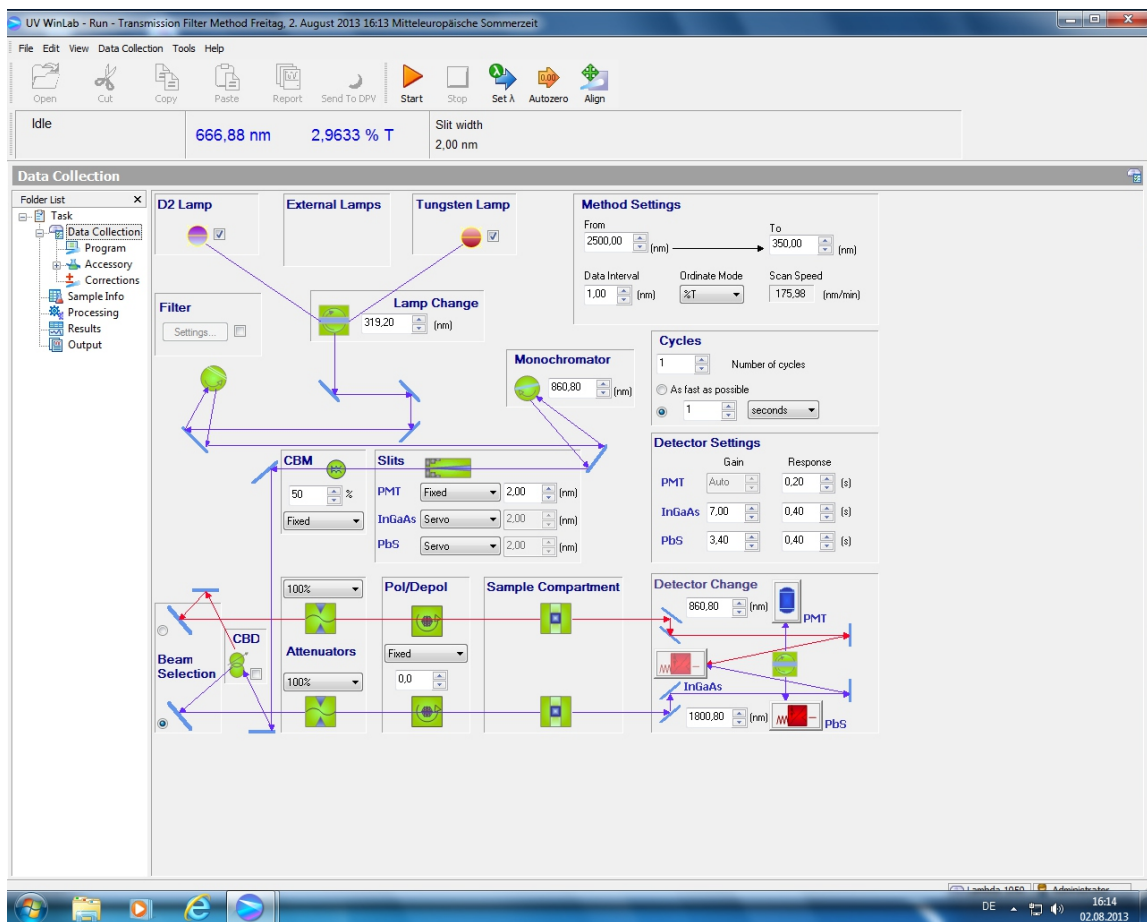


Figure 1.4: UV WinLab Software window for the spectrophotometer settings

In order to get accurate values especially for polarized-radiation sensitive samples the magnitude, kind and direction of polarization of the sample beam must either be known, self-determined or eliminated.

### **Polarization**

It is possible to completely polarize linearly the radiation with the help of a polarizing crystal. Therefore a polarizer drive accessory is installed inside the sample compartment just prior to the sample holder which can be loaded with a polarizing crystal inside the optical path of the sample beam. The crystal can then be turned during the measurement from  $10^\circ$  to  $330^\circ$  via the software. This polarizes the sample beam linearly.

### **Depolarization**

Polarization effects can be reduced with depolarizers. Depolarization is done by Hanle type depolarizers [PE03] They consist of two optical connected crystal wedges. The first one is made of birefringent natural quartz and the second one of synthetic quartz to correct the beam displacement. One depolarizer is placed inside the spectrophotometer. This is the Common Beam Depolarizer (CBD) as shown in figure 1.2. The other one can be placed in the drive accessory in the sample compartment. According to the manufacturer the CBD can reduce polarization by 92%. The crystal inside the drive is able to reduce polarization by 98% [PE03].

## **1.5.2 Homogeneity of detector and light beam**

Neither type of detector can be seen as homogeneous over its entire detecting surface[PE02]. If, due to the sample, the geometry of the light beam changes and the detector is now impinged at a different spot as during the reference measurement, these inhomogeneities could lead to an error. Here, the integrating sphere can be used to eliminate this issue.

Finally the beam itself is inhomogeneous. For compensation it is collimated in width towards the sample position to a minimum of about 1 mm. Outside the spot the light path diverts at an angle of  $3^\circ$  [PE02]. Thus it is important that the sample is fixed exactly at that spot. Additional optics, such as the polarizing crystal, might change the spot position and the beam size and can be a cause of error.

## **1.5.3 Optical paths**

The optical paths of both beams in the spectrophotometer are the same within the limits of manufacturing accuracy[PE02]. Remaining differences are mathematically



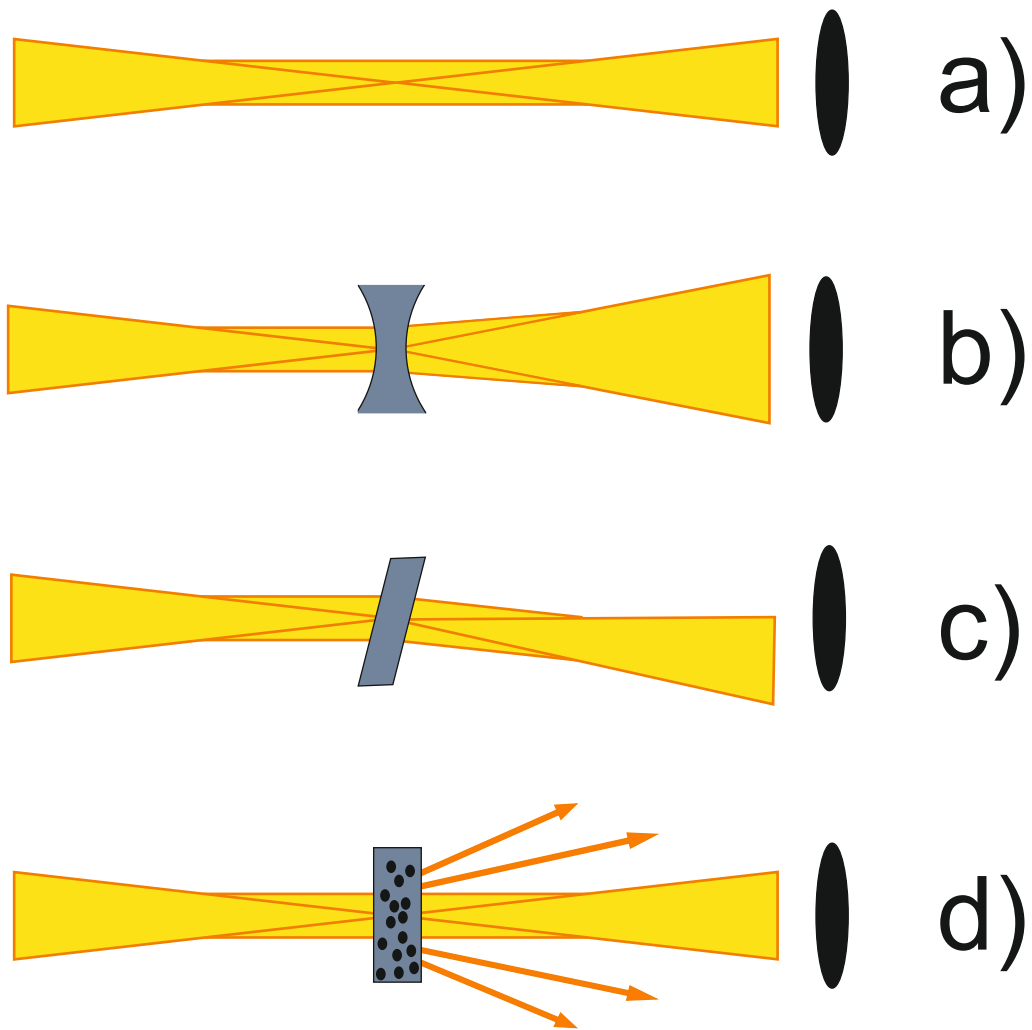


Figure 1.5: This figure shows the variation of the light path due to the insertion of a sample. Case a) is the undisturbed geometry of the light path within the sample compartment. Beams b) to d) are influenced by different samples. Source [PE02]

corrected with the reference measurement. Placing a sample in one light path actually changes it, while the reference path remains unchanged. This could lead to errors, as the sample beam might not hit the detector any more. Figure 1.5 shows in a) the undisturbed light path in the sample compartment and in b) to d) possible alterations of the beam geometry. Cases b) and c) might be optically corrected. The diffuse sample in d) is best placed directly in front of the integrating sphere, as already discussed in section 1.3.

#### 1.5.4 Noise

”There are six different types of noise that afflict the performance of detectors” [RA01] which will not be discussed in detail. Every type of noise is a statistical variation around an average value. The signal to noise ratio can be used as a measure to compare the level of signal to the level of total noise. It is defined as ”the output signal of the detector divided by the standard deviation of this output signal” [KO01]

#### 1.5.5 Aging of the reflection standards

If reflection standards, which are often made out of  $\text{BaSO}_4$  or  $(\text{C}_2\text{F}_4)_n$  are aging, they will reflect less [PE04]. If such a reflection standard is used as base for a reflection measurement, samples will return wrong results. The use of reflection standards is discussed in section 2.3. To ensure high reflectivity, standards must be ground, changed, or recalibrated on a regular basis.

# Chapter 2

## Methods

The following methods were established to get information about the precision of the Perkin Elmer Lambda 1050 Spectrophotometer for transmittance and reflection measurements.

### 2.1 Common Beam Mask

The height of the sample beam, which can be set with the CBM setting in the software was measured in the spectrometer alignment mode. White light is sent through the sample beam and projected on white paper in the sample holder. The height is measured with a calliper gauge.

### 2.2 Transmission measurements

As samples for the transmission measurements a set of 10 glass filters produced by the German manufacturer Schott was used. The dimensions of a glass filter are  $2.1\text{ cm} \times 10.1\text{ cm} \times 0.1\text{ cm}$ . The filter's nominal transmission values (in % T) are: 2.5, 5, 8, 10, 16, 20, 31, 40, 63 and 80. These filters were also measured, by the National Physical Laboratory of the UK (NPL), in % T with an accuracy of three decimals, and were hence used as a reference. The filters were placed on a holder inside the sample compartment which could be horizontally rotated (here called "tilted"). For the transmission measurements the filters had always an angle of  $3^\circ$ , so that the beam did not hit it perpendicularly. For the influence of the angle on the result see section 3.5. The spectrophotometer settings were:

- spectral range: 250 – 2500 nm with measuring points each 1 nm.
- CBM: 50 %, to leave some margin at the upper and lower edges of the filter

- CBD deactivated, as it leads to wrong results, see section 3.1
- the three detector module was used
- slits: fixed at 2 nm for the PMT detector, variable for the infrared detectors, to allow optima intensity levels. As there are no sharp peaks in the filter's spectrum (regarding the dimension of the resolution variation due to the slits), there is no need for a higher resolution.
- signal integration time: 0.2 s PMT, 0.4 s InGaAs, 0.4 s PbS
- detector gain for the infrared detectors: 7 for InGaAs and 3.4 for the PBS

The gain and integrating time settings were found by minimizing the artefacts at the changeover point of the detectors. For more information, see section 3.1.3.

### 2.2.1 Reproducibility

The photometric reproducibility of the Lambda 1050 results is specified by the manufacturer. My measurements were targeted to verify these specifications.

Perkin Elmer used three filters from the United States measurement standard laboratory (National Institute of Standards and Technology, NIST) for repeated transmission measurements. These filters had an absorbance of 1 A, 0.5 A and 0.3 A. The transmittance at Perkin Elmer was measured at a wavelength of 546.1 nm and a slit width of 2 nm. The detector integration time was set to 1 s. Ten measurements were made and the standard deviation out of these results stated in the manual [PE01]

The DLR measurements used the same settings. As sample the 40 % T  $\hat{=}$  0.4 A filter was used and as detector the three detector module. Thereafter another set of measurements was taken with above settings but without any filter to get an impression of the reproducibility of the reference measurement.

### 2.2.2 Polarization

To determine the degree of polarization influence on the transmission results, several polarization measurements were carried out. This was important as the CBD, if activated, significantly distorts the signals (see section 3.1) and is hence deactivated. In all measurements, the polarizing crystal in the drive accessory was used, which is not large enough to cover the largest possible sample beam. To trim the light beam, the CBM was set to 80 % during these measurements.

## CBD

The first measurement determined the capability of the CBD to depolarize light. For this, the polarizing crystal of the accessory drive was used. For the measurement the sample beam passes the depolarizer as well as the polarizing crystal. The crystal is turned from  $200^\circ$  to  $10^\circ$  and the transmittance is measured at  $1^\circ$  intervals. The amplitude of the sinusoidal curve then yields the efficiency of the depolarizer. The beam was set to a wavelength of 500.0 nm and the bandwidth to 2.0 nm .

To avoid polarization effects which are caused by the incidence on the detector, the integrating sphere was used as detector module. Due to the multiple lambertian reflection within the sphere, radiation reaching the detector can be regarded as unpolarized.

## Polarization crystal

In the next measurement the efficiency of the polarization crystal was determined. Therefore, the polarization crystal as well as a polarizing filter (colorPol<sup>®</sup>, optimized for light at 500 nm, from the German manufacturer Codixx) was placed into the sample beam. The crystal was rotated from  $180^\circ$  to  $10^\circ$  and the transmittance was measured. This measurement was again carried out for a fixed wavelength of 500.0 nm with a bandwidth of 2.0 nm.

## Sample Alignment

The last polarization method had the intention to get information about the influence of the tilt of a transmission sample. If polarized light is send through a transmission probe one will find effects on his transmission results depending on the incidence angle and the degree of polarization [TI01]. The 16 % filter was placed in the holder and the holder was rotated to sample beam's incidence angles of  $0^\circ$ ,  $1^\circ$ ,  $5^\circ$  and  $10^\circ$ . As in the above measurements, the polarizing crystal is rotated from  $200^\circ$  to  $10^\circ$  while the transmittance is measured. The wavelength is 500.0 nm and the bandwidth 2.0 nm.

## 2.3 Reflection measurements

The aim of the reflection measurement was to measure the reflectivity of a diffuse reflecting sample. As described in section 1.3 the measurements were done with the sphere module. Figure 2.1 shows the module with the sample holder.

Another difference to transmission measurements is that a reference measurement with 1 R (total reflection) for the detector to calibrate is impossible, as no perfectly lambertian reflector exists. Therefore, a sample of known reflectance must be in the

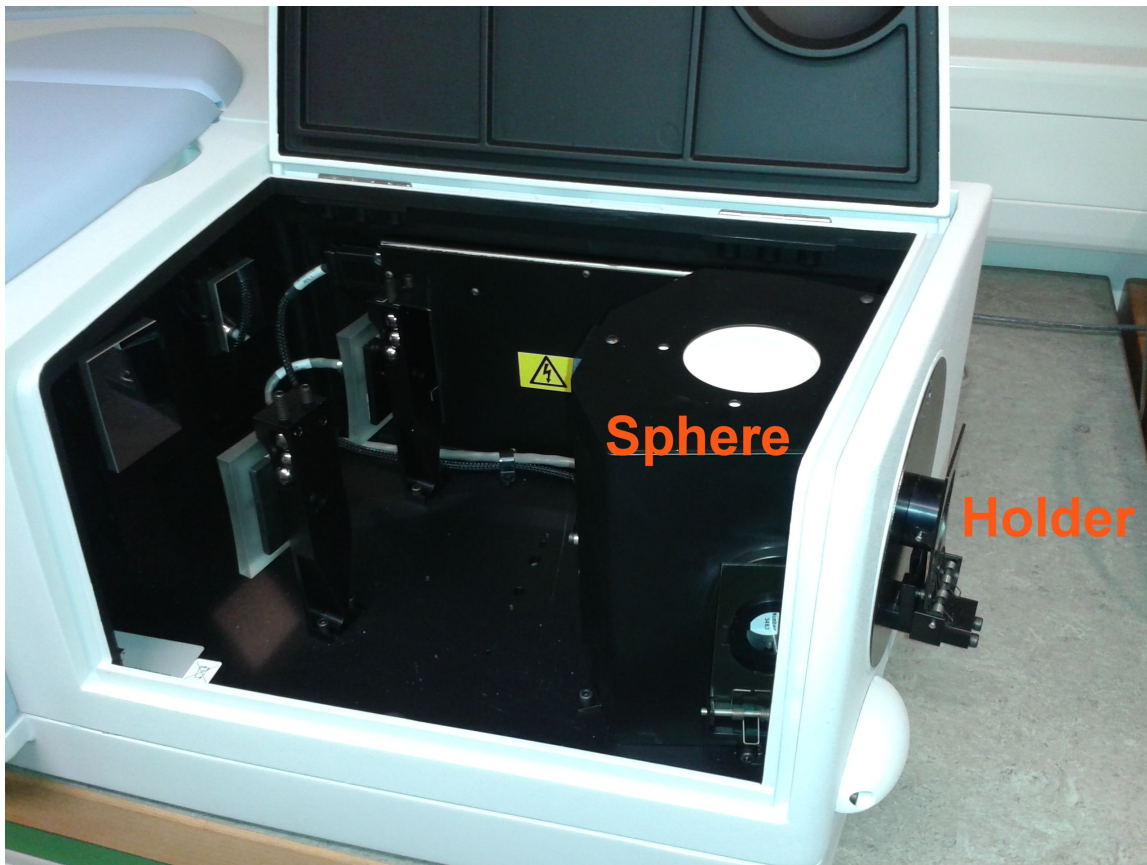


Figure 2.1: Sphere detector module. The sphere is in the right corner with the white opening. The sample is placed at the holder on the right, outside the housing.

sample holder during the reference measurement. For this purpose, a spectralon reflectance target manufactured by the US company Labsphere was used. This reference is provided with a calibration certificate by the US National Institute of Standards and Technology (NIST) and is referenced in this work as "bright spectralon". The results from the calibration certificate are inserted in a .csv file and uploaded by the software, which compares these values during the reference measurement with the measured ones.

Another Labsphere reflectance target with a calibration certificate was used as sample to be able to compare the NIST values with our Lambda 1050 spectrophotometer values. This sample, which has reflectance factors of approximately 0.15 R, is referenced as "dark spectralon".

For the measurement with the sphere module, it is important that both light beams can go unobstructed through the entry ports of the sphere and are not clipped at the edges. The mirrors in front of the sphere on the left side of figure 2.1 could be used for vernier adjustment, if needed. The following spectrophotometer setting were used:

- spectral range: 250 nm to 2500 nm, measurement points every 50 nm
- PMT slit: 2.00 nm, InGaAs slit: variable
- InGaAs gain 17.50
- integration time: PMT: 0.2 s InGaAs: 1.0 s
- CBM 100 %

After the reference measurement with the bright spectralon, both spectralons were measured.





# Chapter 3

## Results

In this chapter the results of my measurements are presented. The chapter begins with a short discussion of my experiences to establish correct methods for reliable results.

### 3.1 Experimental experiences

At the beginning of the measurements during my work at the DLR, the results of the measured filters showed significantly increased values compared to reference values. For an example see figure 3.1. The relative error was for all filters around +4 % T compared with the NPL results. These discrepancies could be traced back to experimental setup problems, which are described below.

#### 3.1.1 Reflection problems

A cause for these high results were multiple reflections within the spectrophotometer. Light reflected by the sample filter was re-reflected either by the safety windows, which protect the optics or by the CBD, being the last optical element of the device before the sample compartment, or by other optical elements along the beam path, compare section 1.3. These reflections led to a multiple transmission and thereby to a bias in the signal. The following steps were performed to significantly reduce this issue:

- Removal of the safety windows.
- Removal of the optional polarizing crystal within the sample compartment.
- Deactivation of the Common Beam Depolarizer within the spectrophotometer by the software.
- Tilt of the sample around  $3^\circ$

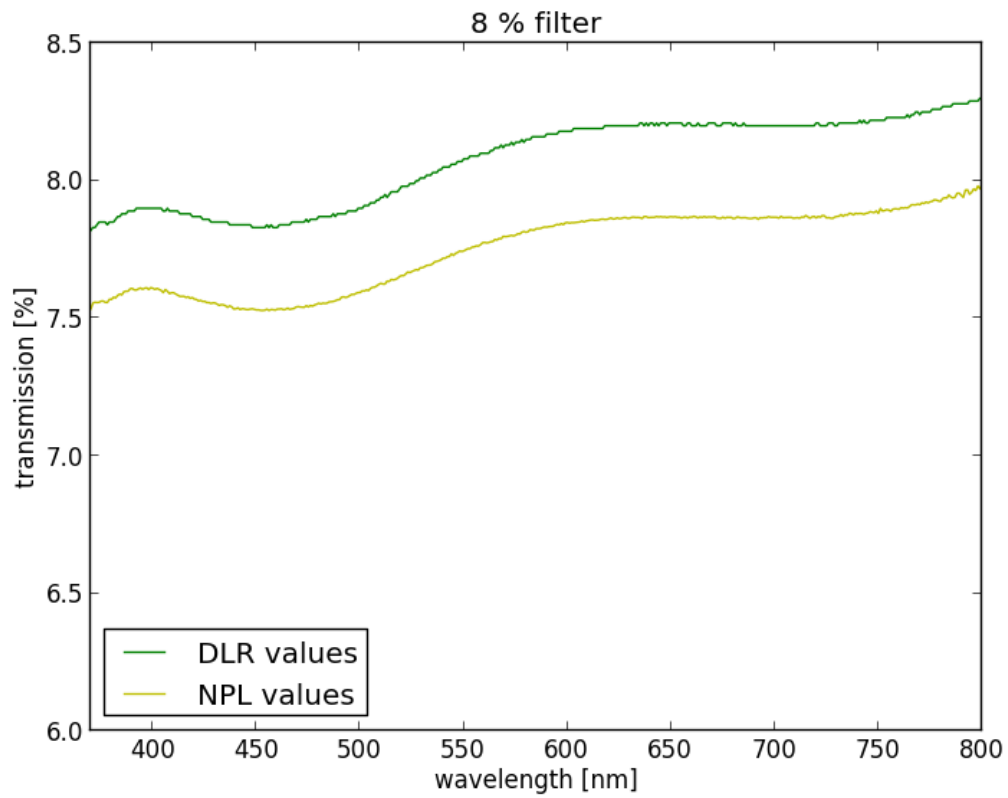


Figure 3.1: 8% filter measurement with a relative error of around 4% compared with the NPL results.

Especially for the last two solutions, it was important to know that the transmission measurements would not be limited by issues connected to the polarization of the beam. As described in section 3.5, this is not the case.

### 3.1.2 Stray light problems

According to the Perkin Elmer customer service, stray light might be another reason for increased transmission results. This stray light might enter the three detector module through a hole, that is needed to connect the detector module with the main spectrophotometer assembly. In our laboratory, no differences could be determined in the measurements after covering the hole.

### 3.1.3 Detector change

During a measurement of the complete spectral range the detector changes twice. The first time at 1800.0 nm and the second time at 880.0 nm. This often introduces artefacts in the measurements, as shown exemplarily in figure 3.2.

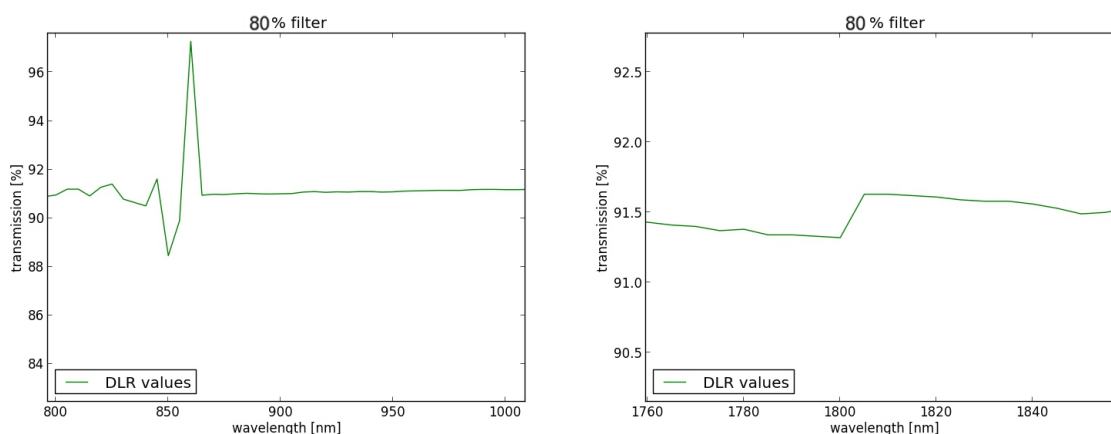


Figure 3.2: Artefacts around the detector change

There are a few causes for these:

- During the detector change the bandwidth of the light changes as well. This is due to the fact that two different types of detectors may need two different energy inputs and the slits are controlled by the software for an optimum intensity level. There is the possibility that the slit is fully open and the maximum width of the slit is reached before the end of one detector's spectral range. Then, at

the wavelength of the detector change, a step is shown in the spectrum. To correct that, the detector gain has to be increased. This enables the slit width to be reduced. The experimenter should strive for an equal slit width at both detectors during the change.

- With the change of the slit, the beam position changes slightly as well. That means that the beam passes the sample at a different spot. As the DLR filter samples are slightly inhomogeneous, this issue can not completely removed. It means, that a little step in the transmission curve might be expected. To reduce this to a minimum, the CBM can be used to trim the spot size, which in turn reduces the energy reaching the detector. Also a mask directly in front of the sample could be used, as long as the mask is completely illuminated throughout the measurement.
- During the detector change, the gratings in the monochromators change as well as described in section 1.3. This affects the polarization of light as can be seen in figure 3.3. For samples sensitive to polarized light, this change can lead to the artefacts. Here the polarization or depolarization options can help.
- If the detector change happens at a wavelength where the spectrum of the sample exhibits a narrow peak of the spectrum, special attention has to be paid to the change of slit width, as the resolution diminishes with a broad slit. The slit width should be at least 0.2% of the peak's half width.

## 3.2 Common Beam Mask

Table 3.1 shows the results of the beam height measurement with an accuracy of  $\pm 0.05$  mm.

Table 3.1: Results of the beam height measurement.

CBM setting (%)	beam height (mm)
100	10.9
75	9.1
50	7.9
25	6.3
10	3.1
0	0.0

As can be seen, the heights are not a linear function of the CBM setting. Moreover, the stated maximum value of 11.7 mm [PE01] can not be set.

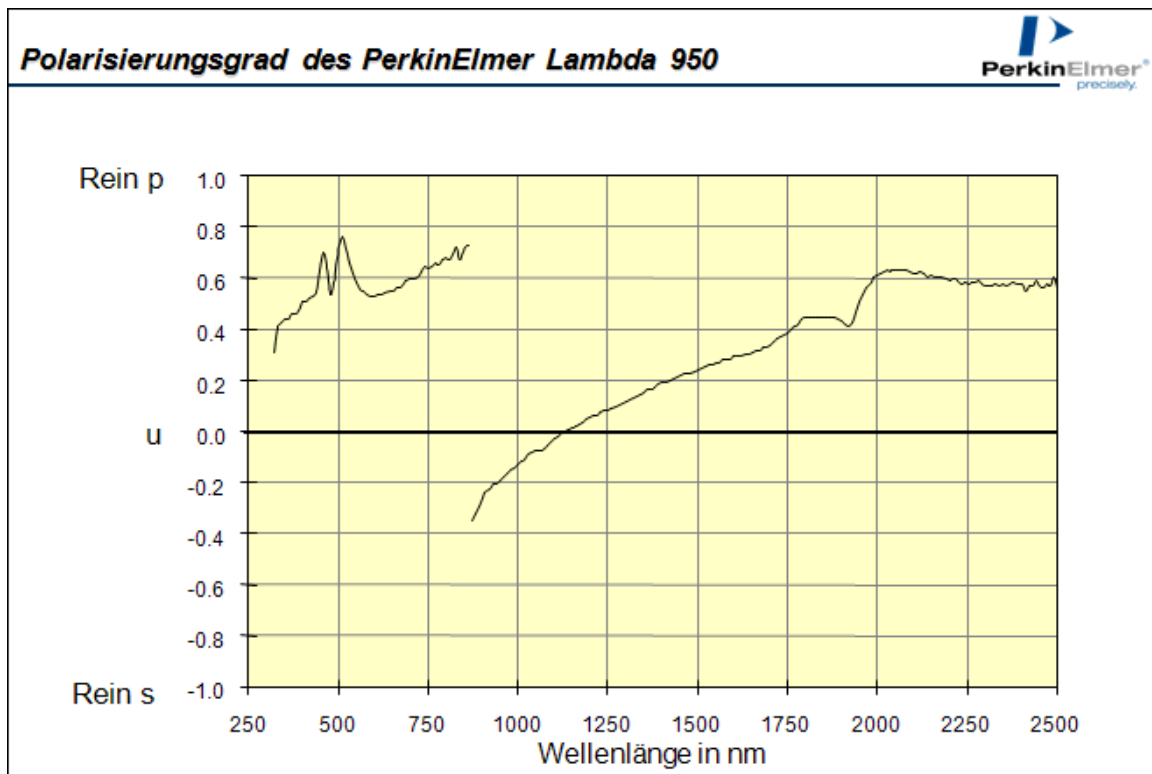


Figure 3.3: Degree of polarisation at the detector change.  $s$  (perpendicular) and  $p$  (parallel) give the direction of the linearly polarized light in relation to the plane of incidence, source [PE04].

### 3.3 Reproducibility of transmittance measurements

Perkin Elmer found the standard deviation out of the results of ten consecutive measurements including ten reference measurements to be  $\leq 0.00016 A$  for an 1 A filter and to be  $\leq 0.00008 A$  for 0.5 A and 0.3 A filters [PE01]. So our 40 % T  $\cong$  0.40 A filter should have resulted in the latter reproducibility.

With the Lambda 1050 spectrophotometer this value could not be reached. The measurements showed a standard deviation of the data of 0.00021 A, which is actually close to three times the stated value.

The set of measurements without sample ( $\cong 0 A$ ) showed a standard deviation of the data of 0.000019 A or 0.05 % T.

Inevitably the sample had to be removed after each measurement out of the sample compartment to allow a new reference measurement. Therefore, small deviations of the position of the beam spot on the sample could not be avoided. Thus, it is assumed that the filters might not be perfectly homogeneous.

To test this assumption, at first ten measurement without removing the sample and therefore without a new reference measurement before the next measurement were made at 546.1 nm for different filters with the same settings as lined out in section 2.2.1. The results were also converted in absorbance A and the standard deviation  $\sigma$  of the results in % T and A was calculated. Table 3.2 shows the results.

Table 3.2: Standard deviation  $\sigma$  of the results of repetitive measurements on a sample without movement of the sample.

filter	$\sigma[\% T]$	$\sigma[A]$
2 %	0.0005	0.0001
16 %	0.00001	0.00003
40 %	0,002	0,00002
80 %	0.003	0.000017
no filter	0.004	0.000016

Apparently this deviation, which might be caused by noise, is dependent on the transmitted light. However all the results are within the above limit. Within one reference measurement cycle, measurements can safely be seen as constant if the sample is not touched.

Next, the influence of the repetitive changing of the sample was measured. During ten measurements within one reference measurement cycle, the above filters were moved intentionally and the influence on the standard deviation  $\sigma$  of these values was noted in table 3.3.

Table 3.3: Repetitive measurements on a sample including movement of the sample.

<b>filter</b>	$\sigma[\% T]$	$\sigma[A]$
2 %	0.013	0.0026
40 %	0.11	0.001
80 %	0.14	0.00066

The errors were at least three times as high as in table 3.2. Consequently the filters can not be assumed to be homogeneous and their error is increasing with nominal values of transmission. Another cause might be the slight uncertainty due to polarization effects, as the glass doesn't fit in perfectly in the holder and small tilt angles of the filter are inevitable, see section 3.5.

Therefore, despite the above reproducibility result of 0.00021 A, the true reproducibility of the spectrophotometer can be rated as being within the specifications. This is further suggested by the set of measurements including reference measurements, without sample.

### 3.4 Filter transmission

After dealing with the experimental experiences from section 3.1 all filters were once more measured for transmission with the method 2.2 and compared to the NPL measurements. For an exemplary comparison, see figure 3.4.

#### Transmission errors

From these results the relative error between the measurements was calculated as shown in figure 3.5.

Finally, for each filter, the mean absolute and relative errors were calculated for the whole range, summarised in table 3.4, as well as for the spectral ranges of each detector summarised in tables 3.5 and 3.6.

To estimate the uncertainty of these results the possible errors shall be estimated. From section 3.3 it is understood that the repetitive changing of the samples is a source of error. In figure 3.6, table 3.3 was plotted as blue points. The green line interpolates between these results. This allows to determine a standard deviation  $\sigma_{mov}$  for the sample movement error at different transmissions.

In table 3.5 and table 3.6 all values which exceed the expected NPL value  $\pm 2 \cdot \sigma_{mov}$  have a light red background. Values which exceed three time the standard deviation have a dark red background, as they might be caused by another issue.

As can be seen for all filters except the 80 % T, the NPL values could be recovered quite well. Regularly repetitions of the 80 % T, did not show any improvement. Hence

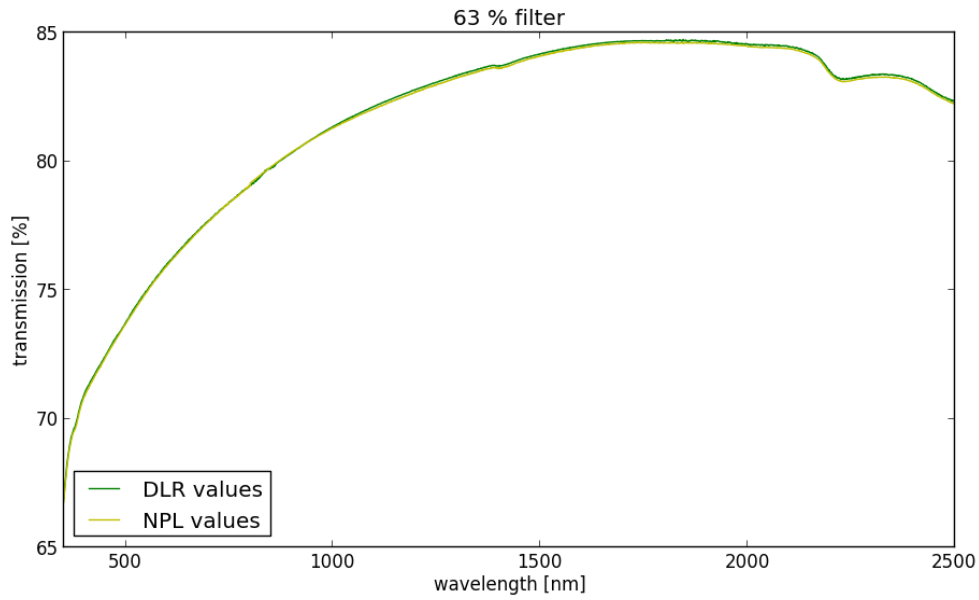


Figure 3.4: Comparison of the transmission values of the 63 % filter.

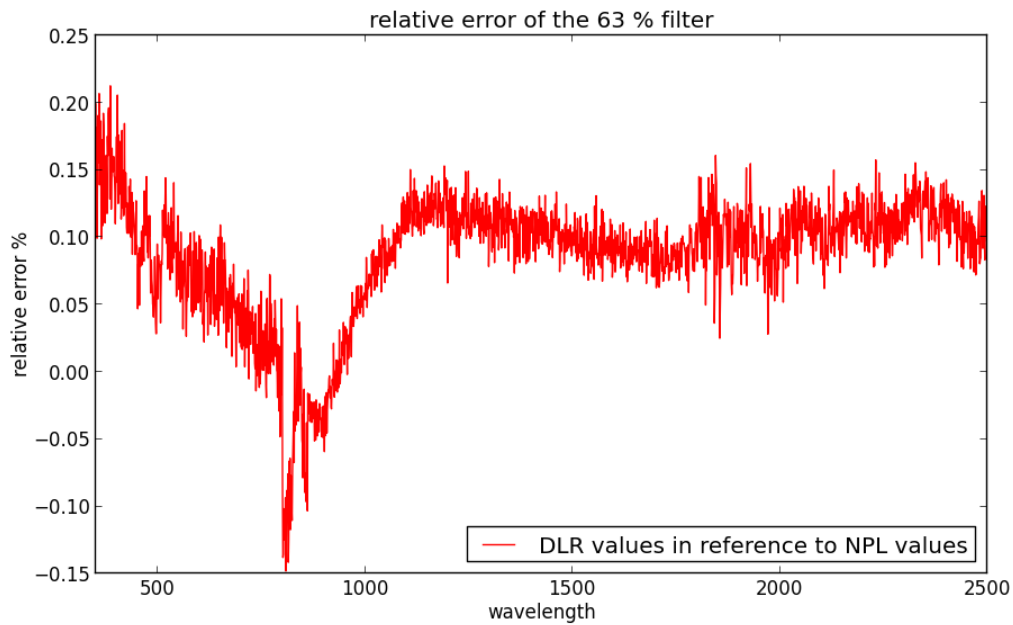


Figure 3.5: Relative error of the 63 % filter' measurements.



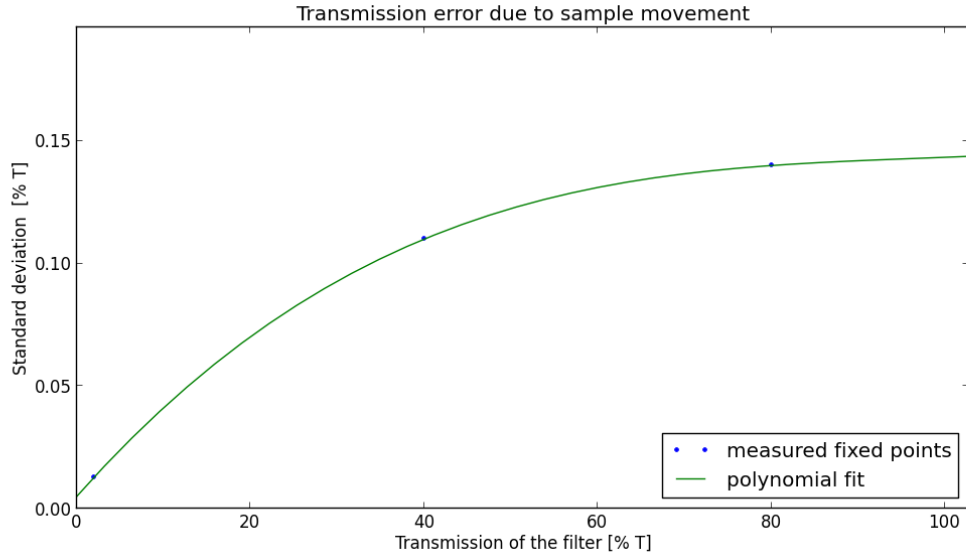


Figure 3.6: Standard deviation  $\sigma_{mov}$  of the error due to sample movements. The green line is a fitted curve through the results of table 3.3 which are plotted as blue points.

Table 3.4: Mean errors of the transmission measurement: absolute errors in % T, relative errors in % without unit.

filter	total error (abs) % T	total error (rel) %
2	-0.017	-0.88
5	-0.017	-0.35
8	-0.024	-0.36
10	0.0082	0.056
16	-0.00053	-0.0049
20	-0.0075	-0.048
31	0.036	0.090
40	0.14	0.33
63	0.071	0.087
80	0.41	0.45

Table 3.5: Mean absolute errors for each detector in % T, values exceeding  $2 \times \sigma_{mov}$  have light red background and values which exceed  $3 \times \sigma_{mov}$  have a dark red background.

filter	error PMT % T	error InGaAs % T	error PbS % T
2.5	0.0061	-0.022	-0.062
5	0.011	-0.016	-0.066
8	-0.0014	-0.025	0.079
10	0.040	0.00053	-0.049
16	0.012	-0.0062	-0.016
20	0.025	-0.019	-0.057
31	0.056	0.0347	-0.0077
40	0.15	0.14	0.12
63	0.048	0.084	0.093
80	0.51	0.355	0.32

Table 3.6: Mean relative errors for each detector in %, cell colors as in table 3.5.

filter	error PMT %	error InGaAs %	error PbS %
2.5	0.28	-1.042	-3.27
5	0.22	-0.38	-1.68
8	0.02	-0.34	-1.22
10	0.38	-0.003	-0.57
16	0.072	-0.038	-0.10
20	0.12	-0.094	-0.322
31	0.14	0.084	-0.020
40	0.35	0.32	0.29
63	0.062	0.10	0.11
80	0.56	0.39	0.36

the filter was measured by a third device, the Cary1, which has been used earlier at the DLR. Figure 3.7 shows the results.

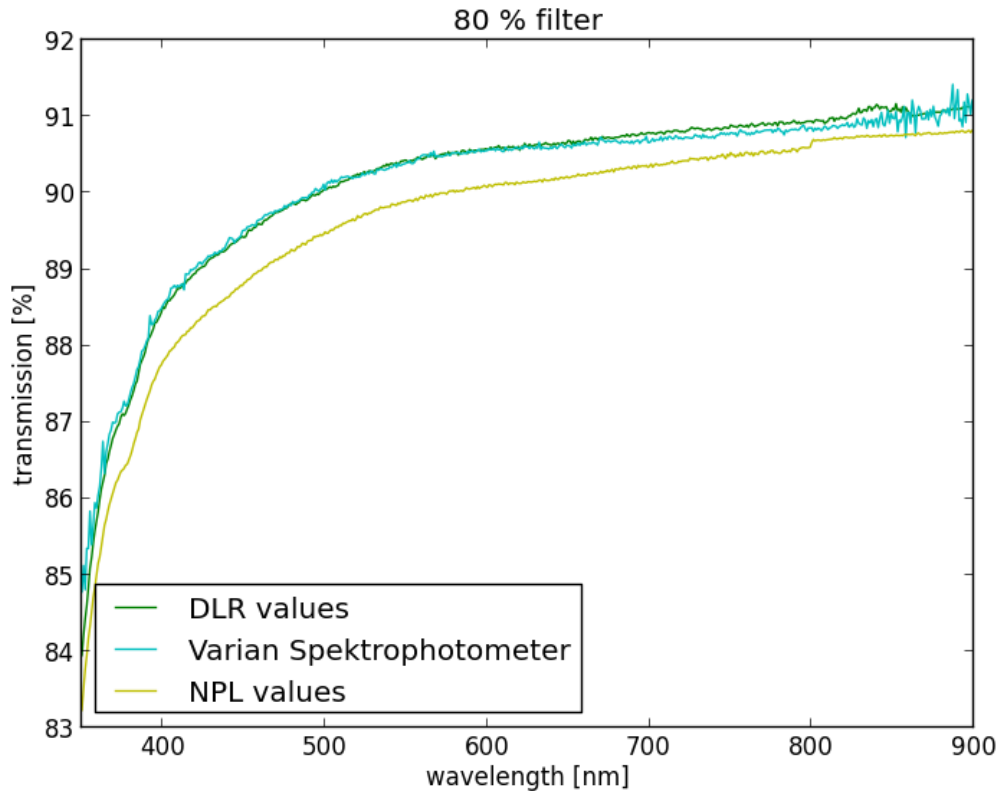


Figure 3.7: 80% Filter measured by the Varian spectrophotometer, compared with NPL and Lambda values.

Clearly, the Varian and Lambda (DLR) values show a higher congruence than the NPL values compared with the Varian values. For this filter it can be concluded that the NPL values are incorrect, indicating that the filter might have aged since the NPL measurement.

Table 3.6 also shows that the PbS detector seems to measure regularly too low results for high-absorbance samples. This issue should be subject of further study.

## 3.5 Polarization

### CBD

The results of the measurements on the depolarisation efficiency of the CBD are shown in figure 3.8. In table 3.7 are the values of the extrema of these transmission curves.

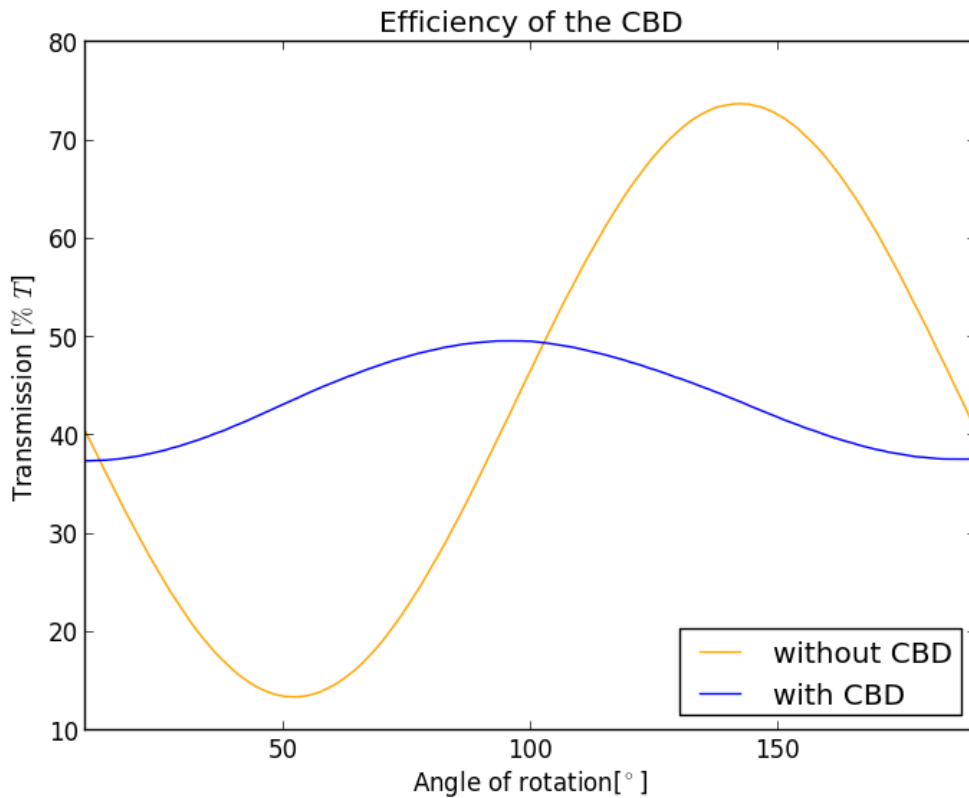


Figure 3.8: Transmission of the polarization crystal.

As can be seen, the CBD has an influence on the polarization of the sample beam. If the CBD worked perfectly, the blue line would just be constant. This is not the case. The amplitude, which shows the extent of polarization, has now been reduced from 28.65% to around 6% which corresponds to a reduction of  $1 - \frac{5.97}{28.56} = 79.1\%$ . This is less than the quoted reduction of 92%.

Table 3.7: Peak values of figure 3.8 ' transmission curves.

	transmission [%] without CBD	transmission [%] with CBD
Maximum	73.76	49.56
Minimum	13.46	37.62
mean transmission	45.11	43.59
amplitude	28.65	5.97

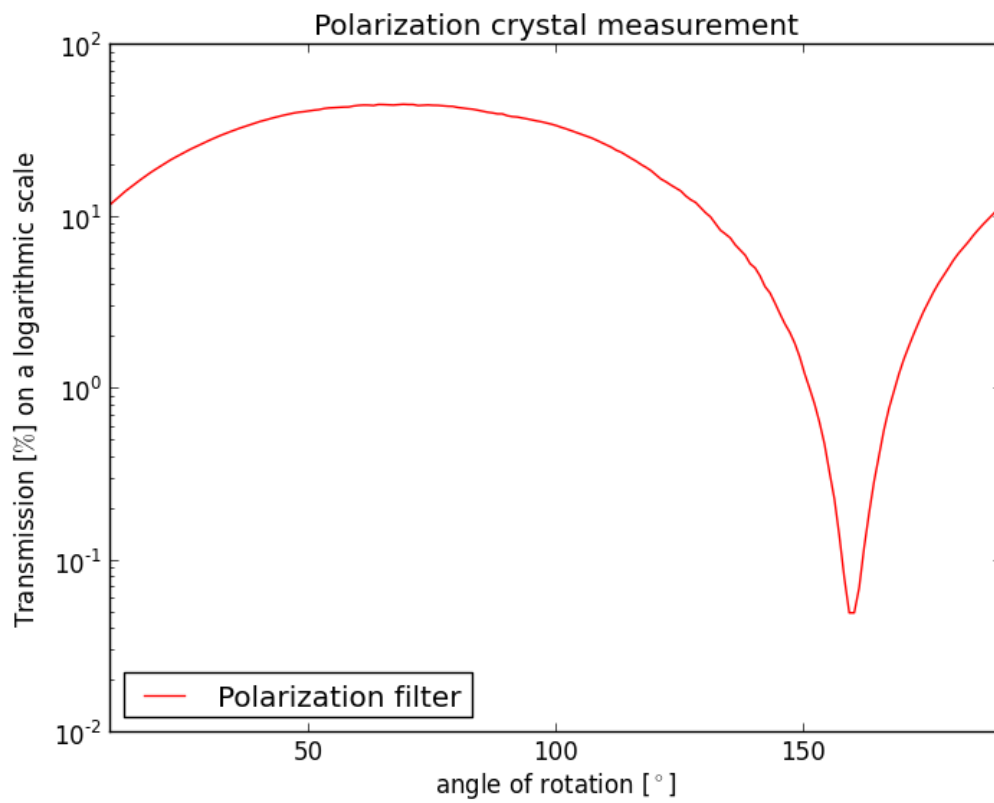


Figure 3.9: Transmission of the crystal in conjunction with a polarizing filter.

### Polarization crystal

The result of the measurement of the polarization crystal is shown in figure 3.9. The plot, which has a logarithmic scale on the transmission axis, shows that the polarizing effect is quite good. The minimum is at a transmission of 0.05%. The remaining transmission might be produced by stray light either generated by the holder of the filter or by the crystal holder, as the quartz crystal does not fit in too well.

### Sample alignment

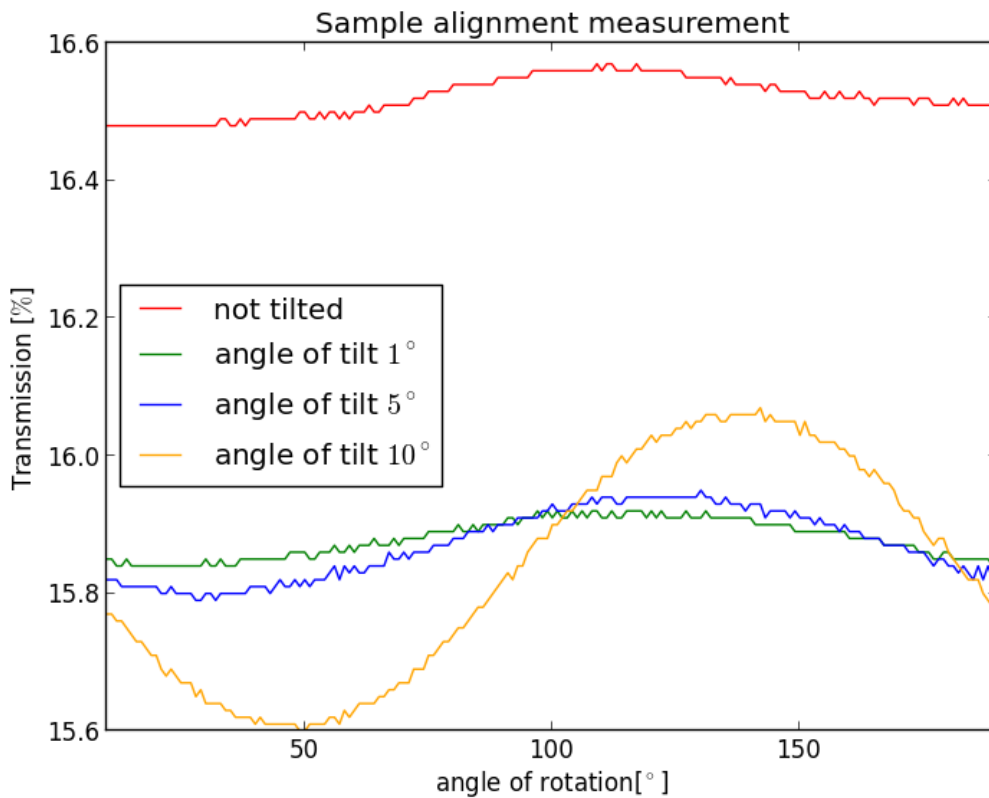


Figure 3.10: Influence of a tilt angle of the filters.

The results of the tilt measurements are shown in figure 3.10. In table 3.8 are the amplitudes of the curves. Two interesting features can be seen. First, as expected, one can see that polarization effects increase with a greater horizontal tilt of the sample, quantified by the amplitude of the sine curve. But even at zero tilt angle we do not see a constant, which is probably due to polarizing effects of the filter glass.

Table 3.8: Results of the sample tilt measurement

Angle of tilt[°]	Amplitude [% T]
0	0.05
1	0.05
5	0.08
10	0.23

Furthermore, one can see the multiple reflection effects at the non-tilted sample. These effects are described above in the section 3.1 and give erroneously high transmission values. This error with an absolute magnitude of  $\Delta T \approx 0.6\%$  is more than ten times bigger than the polarization error due to tilt. Therefore a small tilt of the sample should be accepted.

### 3.6 Reflection measurements

Both samples were measured and the results compared to their calibration certificates. The calculated relative error of the measured values in comparison with the NIST values were plotted in figures 3.11 and 3.12. The mean values were 0.022% for the bright spectralon and -2.89% for the dark spectralon. The good result for the bright spectralon was expected as this one was already used for the reference measurement. This value is actually a result of a reproducibility measurement. The uncertainty, which is in the same dimension as the reproducibility transmission measurements without filter, could be due to noise of the spectrophotometer or inhomogeneity of the sample, as it is reinstalled for the measurement.

The error for the dark spectralon is bigger and must have other reasons. One could be the aging of the samples, as described in section 1.5.5. This is supported by the fact that earlier measurements of this sample even showed higher errors. After cleaning the samples these high errors could be divided in half. Also the aging of the brighter sample could add to the error, because of the measurement procedure with the calibration standard in the sample holder during the reference measurement. If the reflection qualities of the bright spectralon are not as good as stated, the UV WinLab software then refers to these imprecise values.

Looking at figure 3.13, which shows the plotted absolute results of the dark spectralon one can see that the reference values show an artefact (a little step) as in section 3.1.3, which adds to a suddenly greater error in the NIR region. This leads to the assumption that even the reference values might not be as accurate especially in the NIR spectral region. The mean relative error of -2.89% has to be seen in this context. Thus, the established measurement method can be rated as reasonable.

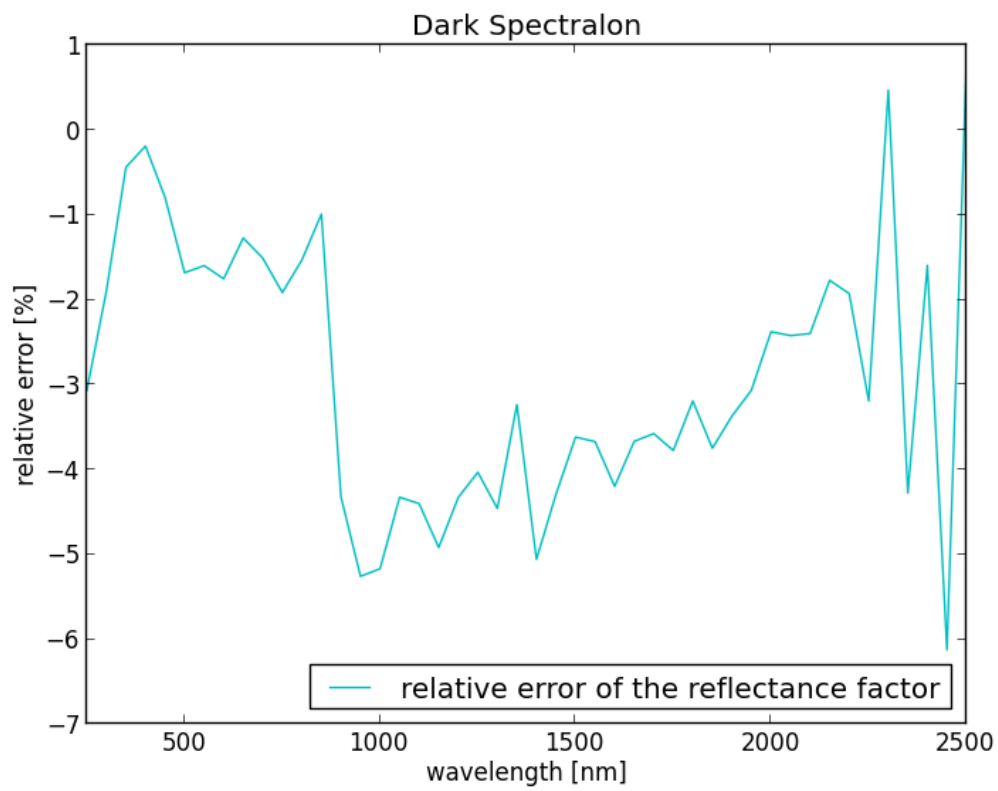


Figure 3.11: Relative error of the measured reflectance factor in comparison with the NIST values for the dark spectralon.



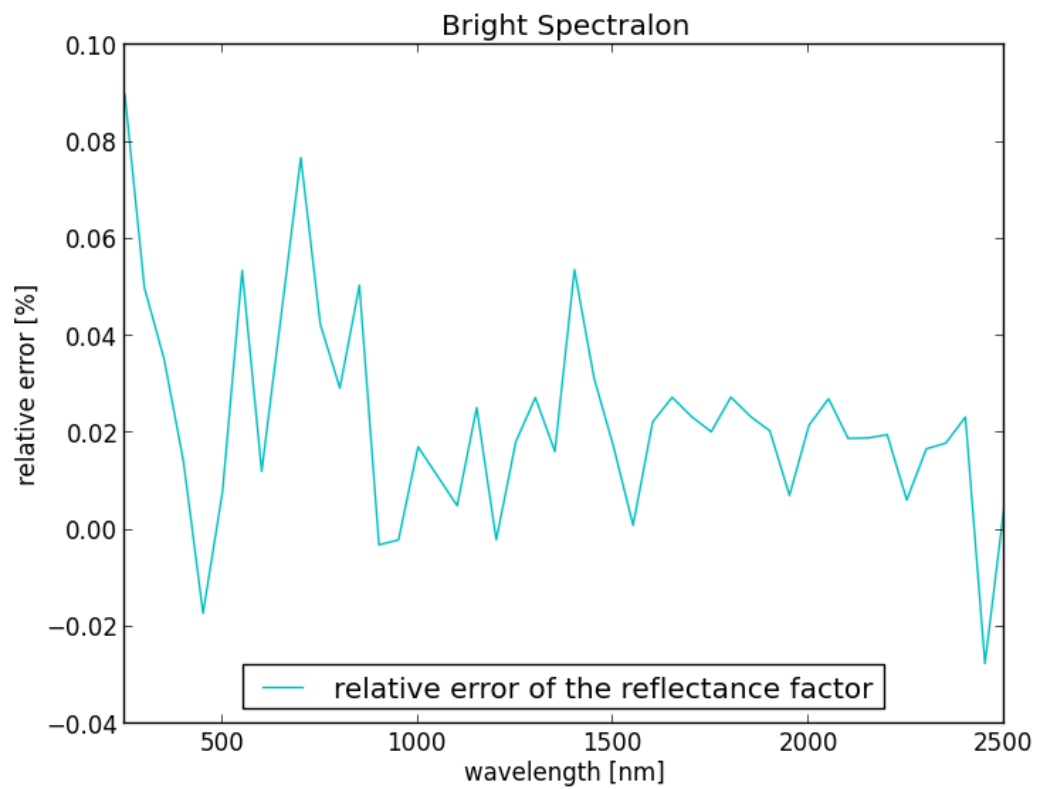


Figure 3.12: Relative error of the measured reflectance factor in comparison with the NIST values for the white spectralon.

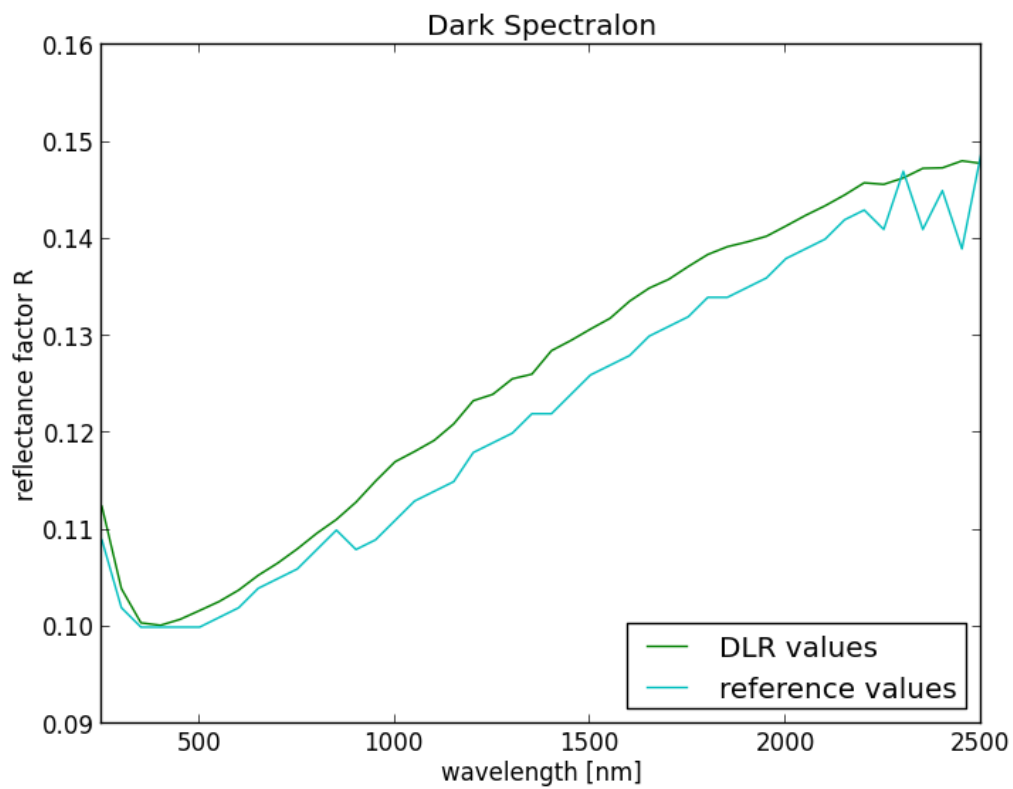


Figure 3.13: Comparison of the measured reflectance factor in with the NIST values for the dark spectralon.

# Chapter 4

## Conclusion & Outlook

In this work methods for transmission and reflection measurements and the results of the characterisation of the Perkin Elmer Lambda 1050 spectrophotometer were presented.

The following conclusions for transmission measurements have been found:

As can be seen from the chapter Results, transmission measurements in a range from 350 nm to 2500 nm can be made with a mean absolute preciseness of 0.06 % T up to 31 % T. For higher transmissions this conclusion is not valid as our reference sample showed inhomogeneities, which exceeded this value. Furthermore the calibration values of the external laboratories don't seem to suit anymore perfectly for the 80% filter. As the old DLR Spectrophotometer Varian Cary 1 showed results for this filter in accordance with the Lambda spectrophotometer these values seem to be more trustworthy than the ones from NPL.

The Spectrophotometer is built to measure absorbance values with the three detector module up to 8 A, but my work only tested it to values  $\approx 1.7A$ . Generally good results were found. Only the PbS detector showed greater errors for higher absorbance values, which reached its maximum at a relative transmission error of 3.3 %. It would be interesting to see if this error is confirmed with different samples.

There were two important results of the method finding process:

One is related to the detector changeover, where the measured spectrum often shows a little artefact. It must be understood, that this artefact is a sign for a measurement method, which is not optimal. Changes in the settings of the method or in the experimental setup should follow in order to minimize this "crack" in the spectrum.

The other result is that multiple reflections between the sample and optics of the spectrophotometer lead to wrong results. These reflections can be avoided by sample tilting, or removing the reflecting optics of the spectrophotometer.

Finally it can be said that the Lambda qualifies as device for measuring calibration standards.



# Bibliography

- [TI01] Tipler P. A., Mosca G. *Physik für Wissenschaftler und Ingenieure*, 2. dt. Auflage, Heidelberg, Elsevier, Spektrum, Akad. Verl. [u.a.], 2006, S.991ff.
- [PE01] Perkin Elmer *High-Performance Lambda Spectrometers Hardware Guide*, Beaconsfield UK; 2007, S.27 & S.77ff.
- [PE02] Perkin Elmer *Tutorial Versatz am Detektorwechsellpunkt*, Rodgau: 2011
- [PE03] Perkin Elmer *Application Note Polarizer/Depolarizer Options for the Lambda 650 and 850 UV/Vis*, Shelton USA; 2003
- [PE04] Perkin Elmer *Tutorial High End Messung mit Kugel*, Rodgau: 2012
- [RA01] William L. Wolfe *Introduction to radiometry*, Bellingham USA, Tutorial Texts In Optical Engineering, Volume TT29, SPIE 1998, S.32f. & S.61ff.
- [KO01] Henry J. Kostkowski *Reliable Spectroradiometry*, La Plata USA: Spectroradiometry Consulting, 1997, S.276ff.
- [LA01] Eichler J., Eichler H.J., *Laser*, 7. Auflage, Berlin: Springer Verlag, 2010
- [GE01] Gege P., Fries J., Haschberger P., Schötz P., Schwarzer H., Strobl P., Suhr B., Ulbrich G., & Vreeling W.J. *Calibration facility for airborne imaging spectrometers*, ISPRS Journal of Photogrammetry and Remote Sensing 64, 2009, S.387ff.
- [SC01] Schaepman M.E., Ustin S.L., Plaza A.J., Painter T.H., Verrelst J., & Liang S. *Earth system science related imaging spectroscopy - An assessment*, Remote Sensing of Environment 113, 2009, S123ff.



# Erklärung

Ich versichere hiermit, dass ich meine Bachelorarbeit selbstständig verfasst und keine anderen als die angegebenen Quellen und Hilfsmittel benutzt habe. Wörtliche oder dem Sinn nach aus anderen Werken entnommene Stellen habe ich unter Angabe der Quellen kenntlich gemacht.

München, den

Valentin Reinhardt